Contribution from the Department of Chemistry,
University of California, Berkeley, California 94720

Structural, Electrochemical, and Magnetic Properties of a Four-Membered Redox Series ($[Cr(L_3)]^{n-}$, n = 0–3) in Catechol–Benzoquinone Complexes of Chromium

STEPHEN R. SOFEN, DAVID C. WARE, STEPHEN R. COOPER, and KENNETH N. RAYMOND*

Received June 28, 1978

The complexes tris(3,5-di-*tert*-butyl-*o*-benzoquinone)chromium(0) and potassium tris(3,5-di-*tert*-butylcatecholato)chromate(III) have been isolated. Electrochemical techniques have demonstrated these complexes to be members of a reversible three-electron redox series with formal reduction potentials of +0.03, −0.47, and −0.89 V vs. SCE in acetonitrile. The four members of this series have been characterized by visible, infrared, and EPR spectroscopies as well as by cyclic voltammetry and magnetic susceptibility. From 4.3 to 298 K the neutral complex is diamagnetic. The mono-, di-, and trianion have, respectively, 1, 2, and 3 unpaired electrons. The EPR spectrum of the monoanion consists of a signal centered at g = 1.98 with 8-G line width and coupling to the metal of 24.3 G. The neutral complex has spontaneously resolved upon crystallization to the Λ-cis isomer in space group $R3$ with a = 16.385 (3) Å, c = 13.874 (4) Å, d(exptl) = 1.08 g cm^{-3}, and d(calcd) = 1.11 g cm^{-3} for Z = 3. The crystallographic symmetry of the molecule is C_3 while the symmetry of the coordination polyhedron is D_3. The ligand structure in the neutral complex retains significant quinone character; the C–O bond length is 1.285 (8) Å and there is an alternation in the C–C bond lengths of the ring which range from 1.370 (10) to 1.433 (9) Å. The Cr–O bond length is 1.933 (5) Å. The structural results are compared to those of the trianion, tris(catecholato)chromate(III), in which the ligand retains an undistorted catechol geometry.

Introduction

As part of our interest in microbial iron transport agents, we have previously reported the synthesis and structural characterization of the tris(catecholato)chromate(III) and -ferrate(III) ions.[1] Observations of the reactions of molecular oxygen with these and other catechol chelate complexes as well as our interest in the mechanism of metal ion release in the tricatechol siderophore enterobactin led to our investigations of the redox properties of chromium complexes of catechols and oxidized catechols (*o*-benzoquinones).

Catechol is a non-innocent ligand which is a terminal member of the redox series catecholate (**1**), *o*-benzosemiquinone (**2**), and *o*-benzoquinone (**3**). Thus, metal complexes of catechol might reasonably be expected to be members of the electron-transfer series **4**–**7** similar to the dithiolene and *o*-benzoquinone diimine systems.[2,3] Square-planar complexes of divalent metals were investigated earlier in this light by Röhrscheid, Balch, and Holm.[4] More recently, Pierpont and co-workers have prepared six-coordinate complexes of tetrachloro- and phenanthrenequinone with group 6B metals.[5,6] Also, Razuvaev et al. have reported the synthesis of several metal complexes using the 3,5-di-*tert*-butylcatechol ligand.[7] Balch and also Brown have investigated oxidative addition reactions of a single quinone to metal complexes.[8,9] Among these structural studies are compounds characterized as having coordinated hydroquinone (catechol), semiquinone, and quinone ligands. It was of interest to us to elaborate further the electrochemical properties of such chelates as well as to characterize structurally complexes where the ligand lacked electron-withdrawing substituents.

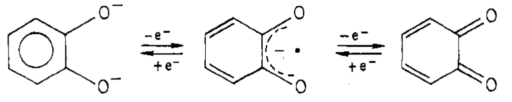

1 **2** **3**

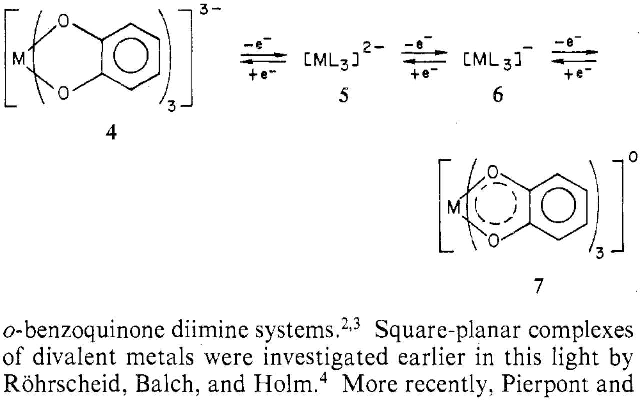

4 **5** **6** **7**

Due to the thermal instability of unsubstituted *o*-benzoquinone with respect to polymerization, our initial work focused on 3,5-di-*tert*-butyl-substituted catechol and quinone. In the dithiolene series, the more reduced tris chelates show a tendency to adopt octahedral coordination rather than the trigonal-prismatic geometry observed for more oxidized dithiolene complexes.[10] It was hoped that using the more electron-rich di-*tert*-butylquinone would permit formation of a more readily oxidized chelate. Finally, it was of interest what effect the elimination (by bulky *tert*-butyl groups) of close intermolecular contact[5] would have on the structural and magnetic properties of these complexes. Here we report our results on the structural, magnetic, spectroscopic, and redox properties of the chromium–3,5-di-*tert*-butylcatechol system.

Experimental Section

Compound Preparation. Reagent grade materials were used as purchased with the following exceptions. Acetonitrile used in electrochemistry was dried and purified by distillation, sequentially, from calcium hydride, phosphorus pentoxide, and calcium hydride. Tetrahydrofuran (THF) was distilled from sodium–benzophenone ketyl prior to use. Tetraethylammonium perchlorate was recrystallized at least twice. Due to the oxygen sensitivity of catechol anions, all experimental manipulations were carried out on a Schlenk line or in a recirculating atmosphere drybox under O_2-free nitrogen or argon. All solvents were deoxygenated before use. Analyses were performed by the Microanalytical Laboratory, University of California, Berkeley.

$K_3[Cr(O_2C_{14}H_{20})_3]\cdot 6H_2O$. Ten milliliters of an aqueous solution of 1.33 g of $CrCl_3\cdot 6H_2O$ (5 mmol) was added to an aqueous solution of 3.56 g of 3,5-di-*tert*-butylcatechol (16 mmol) and 1.85 g of KOH (33 mmol). The green precipitate product was washed twice with cold water and once quickly with ice cold acetone. The compound is soluble in most common organic solvents. Anal. Calcd for $K_3[Cr(O_2C_{14}H_{20})_3]\cdot 6H_2O$ (M_r = 934.4): C, 53.75; H, 7.75; K, 12.5; Cr, 5.54. Found: C, 52.91; H, 7.08; K, 13.0; Cr, 5.29.

$Cr(O_2C_{14}H_{20})_3$. In a 100-mL flask, 3.75 g of 3,5-di-*tert*-butyl-*o*-benzoquinone (17 mmol) and 1.25 g of $Cr(CO)_6$ (5.7 mmol) were heated under reflux in 50 mL of diglyme. (Lower boiling solvents gave no product.) In initial experiments the volume of CO evolved was monitored and found to stop after 6 equiv were liberated (3 h). The solution was concentrated and cooled to −15 °C. The crystalline product was washed with cold acetone and dried under vacuum. The complex is readily recrystallized from hydrocarbon solvents and may also be prepared by UV photolysis (30 min) in THF or toluene at or below room temperature. Anal. Calcd for $Cr(O_2C_{14}H_{20})_3$ (M_r = 713.0): C, 70.74; H, 8.50; Cr, 7.29. Found: C, 70.29; H, 8.42; C, 7.13.

Physical Measurements. Magnetic susceptibilities were determined by the Evans method[11] using a $NiCl_2/C_3H_6O$ calibrant and either a Varian A-60 or T-60 spectrometer at 25 or 35 °C, respectively. The

0020-1669/79/1318-0234$01.00/0 © 1979 American Chemical Society

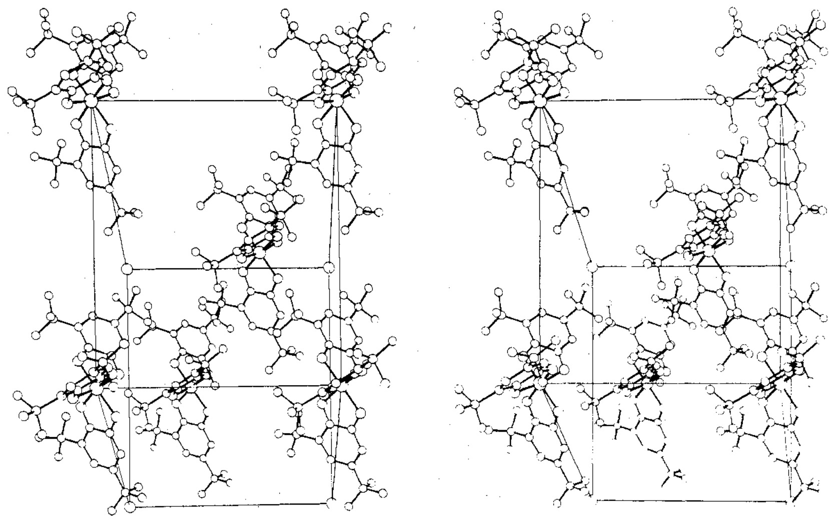

Figure 1. Stereoscopic packing diagram of the neutral complex of 3,5-di-*tert*-butyl-*o*-benzoquinone and chromium viewed along the crystallographic *b* axis. (The trigonal axis, *c*, is horizontal.)

room-temperature susceptibility of the neutral complex was determined on a standard Gouy balance. The low-temperature (4.3–49.1 K) susceptibility of this complex was determined with a PAR Model 155 vibrating-sample magnetometer used with a homogeneous magnetic field produced by a Varian 12-in. electromagnet. Measurements were made at field strengths of 12.5, 10.0, 7.5, and 5.0 kG on two separate samples. The magnetometer was calibrated using $HgCo(SCN)_4$.[12] Susceptibilities were corrected for the diamagnetism of the Kel-F sample holder.[13] Due to the problems in using Pascal's constants on quinone/semiquinone ligands, no correction was made for the underlying sample diamagnetism.[14]

All electrochemical experiments were carried out using the three-electrode configuration in rigorously dry, O_2-free acetonitrile with 0.1 M tetraethylammonium perchlorate electrolyte. A platinum disk (for cyclic voltammetry) or platinum mesh (for preparative electrolysis) working electrode and a Pt-wire auxiliary electrode were used. The reference electrode was either a saturated calomel electrode (SCE) or, for experiments conducted in the drybox, a $Ag/AgNO_3$ (0.1 M) electrode. The instrumentation used included a PAR Model 175 universal programmer, a Model 173 potentiostat, and a Model 179 coulometer.

The EPR spectra were recorded on Varian E-9 or E-3 X-band spectrometers in serum-capped quartz cells using acetonitrile solvent at 298 and 77 K. Infrared spectra were recorded as hydrocarbon or fluorocarbon mulls using NaCl or KBr plates on either a Perkin-Elmer 337 or 597 spectrophotometer. Electronic absorption spectra were recorded on Cary Model 17 and Model 118 spectrophotometers.

Unit Cell and Diffraction Data. Crystals of the neutral complex suitable for X-ray diffraction were obtained by slow evaporation of hexane solutions or slow cooling of hot, saturated octane solutions. A preliminary search of low-angle reflections on the CAD-4 diffractometer gave a trigonal unit cell. Subsequent precession photographs revealed Laue symmetry $\bar{3}$ and systematic absences hkl, $-h + k + l = 3n$. The subsequent solution and refinement of the structure confirmed that the space group is the acentric group $R3$.[15] Crystal data obtained by a least-squares fit to 25 high-angle reflections are given in Table I.

Intensity data were collected on a Nonius CAD-4 automated diffractometer using monochromatic Mo Kα radiation.[16–18] The data were processed with a parameter, p, introduced to prevent overweighting strong reflections, chosen as 0.03.[19] Due to the small variation in transmission coefficients, no correction for absorption was applied. Crystal density was determined by flotation in octane/carbon tetrachloride and also in $H_2O/ZnBr_2$ and found to be 1.08 (2) g cm^{-3} compared to a calculated value of 1.10 g cm^{-3}.

Structure Determination. Positions for the chromium, oxygens, and phenyl carbons were deduced from a sharpened Patterson map, and these led to completion of the structure by standard difference Fourier and least-squares techniques. Full-matrix refinements were employed using 1192 independent reflections with $F_o^2 > 3\sigma(F_o^2)$.[20–23] Of the 20 unique hydrogens, 13 could be located with certainty; however, all hydrogens were entered at fixed, calculated positions with isotropic temperature factors of 7.0 Å^2 for the two ring hydrogens and 10.0 Å^2 for the *tert*-butyl hydrogens. Positions for the two ring hydrogens were calculated assuming that the C–H bond bisects the C–C–C angle of the ring and that the C–H bond distance is 0.95 Å.[24] The *tert*-butyl hydrogens were entered as three-membered rigid groups calculated for each tetrahedral methyl group with the methyl C atom's coordinates serving as the group origin. These rigid groups were allowed to rotate about the C–C bond during refinement. Examination of the final difference map showed no peak greater than 0.1 e/Å^3. The final unweighted (R) and weighted (R_w) agreement factors are 5.6 and 6.48, respectively,[25] and the error in an observation of unit weight is 1.9. Refinement of the alternate enantiomorph gave R = 8%. Table II gives the positional and thermal parameters of the nonhydrogen atoms. Table III gives the final positional parameters for the fixed hydrogen atoms and Table IV lists the amplitudes of vibration derived from the thermal parameters.[26]

Table I. Summary of Crystal Data for $Cr[O_2C_6H_2(C_2H_9)_2]_3$

mol wt 713.02
hexagonal setting
space group $R3$
cell constants,[a] Å
a = 16.385 (3)
c = 13.874 (4)
formula units/cell = 3

cell vol = 3235 Å^3
Mo Kα radiation
μ = 3.0 cm^{-1}
d(exptl) = 1.08 g cm^{-3}
d(calcd) = 1.11 g cm^{-3}
crystal size =
0.27 × 0.25 × 0.40 mm

[a] Ambient temperature of 26 °C.

The crystal structure consists of three discrete CrL_3 molecules per rhombohedral cell in the hexagonal setting which lie on crystallographic threefold axes (Figure 1). Intermolecular interactions in the crystal are weak, due to the large *tert*-butyl groups, which preclude the type of π stacking observed in the phenanthrene- and tetrachloroquinone complexes.[5] The weak packing forces result in large thermal motion of the *tert*-butyl groups.

The coordination geometry of the complex closely corresponds to D_3 point symmetry. Individual CrL_3 molecules (Figure 2) are trigonally distorted octahedral complexes which have spontaneously resolved into the Λ-cis isomer upon crystallization. The ring O–M–O angle is reduced to 81.4 (2)° from 90° for an octahedron. The trigonal twist angle of the top trigonal face relative to the bottom is 48.6 (2) vs. 60° for an octahedron.[27] The δ shape parameters of Muetterties and Guggenberger[28] are 61.8 (2), 80.4 (2), 70.0 (2), and 70.5 (1)°. The corresponding values for an ideal trigonal prism are 0, 120, 90, and 90°. In an ideal octahedron all of the dihedral angles equal 70.5°.

Average bond lengths and angles are shown in Figure 3, where they are compared with the tris(catecholato)chromate(III) complex. Individual bond lengths and angles are presented in Table V. The average Cr–O bond length, 1.932 (5) Å, is shorter than in the $[Cr(cat)_3]^{3-}$ anion [average 1.986 (4) Å].[1,29] The Cr–O bond distances in some other complexes are 1.951 (6) Å in $Cr(acac)_3$,[30] 1.96 (4) Å in $Cr(ox)_3^{3-}$,[31] and 1.949 (5) Å in $Cr(Cl(quin))_3$.[5,29] Carbon–carbon distances in the 3–4 and 5–6 bonds are significantly shorter than the

Table II. Positional and Thermal Parameters (×10^4) for the Nonhydrogen Atoms in $Cr[O_2C_6H_4(C_2H_9)_2]_3$

atom	x	y	z	β_{11}[a]	β_{22}	β_{33}	β_{12}	β_{13}	β_{23}
Cr[b]	0	0	0	54.0 (8)[c]	54.0 (0)	57.9 (9)	27.0 (4)	0	0
O_1	0.0986 (4)	0.0982 (4)	0.9223 (3)	58 (4)	75 (4)	60 (3)	34 (3)	−2 (3)	17 (3)
O_2	0.1068 (3)	0.0221 (3)	0.0771 (3)	53 (3)	44 (3)	62 (4)	22 (3)	8 (3)	15 (2)
C_1	0.1814 (6)	0.1296 (4)	0.9568 (5)	63 (5)	43 (4)	58 (4)	25 (4)	16 (4)	15 (3)
C_2	0.1877 (5)	0.0879 (5)	0.0452 (4)	57 (5)	49 (4)	50 (4)	30 (4)	3 (4)	−1 (3)
C_3	0.2763 (5)	0.1159 (4)	0.0888 (5)	62 (5)	41 (4)	62 (4)	20 (4)	−8 (4)	−5 (4)
C_4	0.3530 (5)	0.1835 (6)	0.0402 (6)	68 (6)	68 (5)	77 (5)	28 (5)	−9 (4)	−7 (5)
C_5	0.3495 (6)	0.2272 (5)	0.9539 (7)	72 (6)	45 (5)	116 (7)	22 (4)	30 (5)	20 (4)
C_6	0.2632 (6)	0.2001 (6)	0.9132 (5)	87 (7)	75 (5)	69 (5)	49 (5)	8 (5)	16 (4)
C_7	0.2825 (6)	0.0716 (6)	0.1834 (6)	69 (5)	60 (5)	86 (6)	25 (4)	−20 (4)	−5 (4)
C_8	0.2391 (15)	0.105 (2)	0.2614 (8)	288 (19)	193 (24)	80 (6)	133 (20)	−55 (9)	−37 (8)
C_9	0.229 (2)	0.9641 (16)	0.1737 (9)	176 (13)	102 (10)	144 (9)	76 (9)	−53 (9)	2 (7)
C_{10}	0.3846 (11)	0.1085 (12)	0.2081 (12)	125 (10)	171 (11)	265 (17)	37 (9)	−119 (11)	82 (12)
C_{11}	0.4422 (7)	0.3034 (8)	0.9054 (7)	81 (7)	99 (7)	133 (8)	43 (6)	45 (6)	30 (6)
C_{12}	0.516 (3)	0.358 (2)	0.9668 (16)	282 (34)	386 (40)	244 (20)	224 (29)	−21 (23)	22 (24)
C_{13}	0.4215 (16)	0.3502 (14)	0.8287 (19)	201 (19)	185 (18)	363 (27)	92 (16)	163 (19)	191 (20)
C_{14}	0.4777 (17)	0.2436 (18)	0.864 (3)	251 (26)	220 (23)	758 (67)	136 (22)	383 (40)	239 (35)

[a] The form of the anisotropic thermal ellipsoid is $\exp[-(\beta_{11}h^2 + \beta_{22}k^2 + \beta_{33}l^2 + 2\beta_{12}hk + 2\beta_{13}hl + 2\beta_{23}kl)]$. [b] Located on the crystallographic threefold axis at 0, 0, 0. [c] Standard deviations of the least significant figures are given here and elsewhere in parentheses.

Table III. Position Parameters for the Fixed Hydrogen Atoms[a]

atom	x	y	z
H_4	0.4135	0.2029	0.0667
H_6	0.2590	0.2295	0.8559
H_{8a}	0.1788	0.0992	0.2446
H_{8b}	0.2807	0.1680	0.2862
H_{8c}	0.2300	0.0590	0.3103
H_{9a}	0.2658	−0.0563	0.1371
H_{9b}	0.1690	−0.0568	0.1415
H_{9c}	0.2174	−0.0629	0.2379
H_{10a}	0.4087	0.1759	0.2073
H_{10b}	0.4062	0.0906	0.1510
H_{10c}	0.4074	0.0920	0.2652
H_{12a}	0.4994	0.3962	0.0043
H_{12b}	0.5705	0.3982	−0.0744
H_{12c}	0.5350	0.3224	0.0094
H_{13a}	0.3622	0.3035	−0.2000
H_{13b}	0.4715	0.3696	−0.2185
H_{13c}	0.4168	0.4045	−0.1513
H_{14a}	0.5379	0.2861	−0.1658
H_{14b}	0.4330	0.2052	−0.1856
H_{14c}	0.4855	0.2032	−0.0905

[a] The subscript of each hydrogen atom is chosen to be the same as the carbon atom to which it is bonded. The isotropic temperature factor for H_4 and H_6 is 7.0 and 10.0 Å^2 for the remaining atoms.

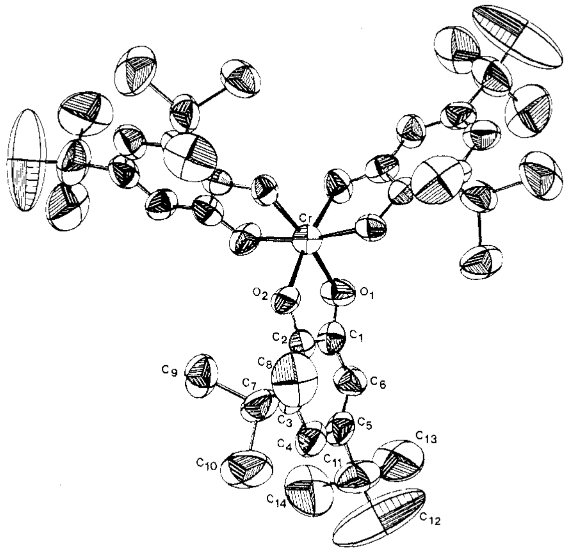

Figure 2. ORTEP drawing of the neutral complex of 3,5-di-*tert*-butyl-*o*-benzoquinone and chromium viewed down the crystallographic *c* axis. The individual atoms are drawn at 50% probability contours of the thermal motion. Hydrogen atoms are omitted for clarity.

Table V. Bond Distances and Angles in $Cr[O_2C_6H_2(C_2H_9)_2]_3$

Distances, Å

Cr–O_1	1.940 (5)	C_3–C_7	1.529 (10)
Cr–O_2	1.925 (5)	C_7–C_8	1.54 (3)
O_1–C_1	1.280 (8)	C_7–C_9	1.53 (3)
O_2–C_2	1.299 (8)	C_7–C_{10}	1.51 (2)
C_1–C_2	1.433 (9)	C_5–C_{11}	1.555 (12)
C_2–C_3	1.420 (9)	C_{11}–C_{12}	1.38 (3)
C_3–C_4	1.366 (10)	C_{11}–C_{13}	1.45 (2)
C_4–C_5	1.411 (11)	C_{11}–C_{14}	1.48 (3)
C_5–C_6	1.374 (10)		
C_6–C_1	1.395 (10)		

Angles, Deg

O_1–Cr–O_2	81.4 (2)	C_2–C_3–C_7	120.8 (6)
Cr–O_1–C_1	113.7 (4)	C_3–C_7–C_8	106 (1)
Cr–O_2–C_2	114.9 (4)	C_3–C_7–C_9	109.5 (7)
O_1–C_1–C_2	116.3 (5)	C_3–C_7–C_{10}	109.2 (8)
O_1–C_1–C_6	123.8 (6)	C_8–C_7–C_9	112 (1)
O_2–C_2–C_1	113.6 (6)	C_8–C_7–C_{10}	108 (1)
O_2–C_2–C_3	125.6 (6)	C_9–C_7–C_{10}	111 (1)
C_1–C_2–C_3	121.0 (6)	C_4–C_5–C_{11}	121.0 (8)
C_2–C_3–C_4	115.4 (6)	C_5–C_{11}–C_{12}	116 (1)
C_3–C_4–C_5	125.2 (7)	C_5–C_{11}–C_{13}	110 (1)
C_4–C_5–C_6	118.7 (6)	C_5–C_{11}–C_{14}	100.7 (9)
C_5–C_6–C_1	119.8 (6)	C_{12}–C_{11}–C_{13}	118 (2)
C_6–C_1–C_2	119.9 (7)	C_{12}–C_{11}–C_{14}	100 (3)
		C_{13}–C_{11}–C_{14}	110 (2)

Table VI

Weighted Least-Squares Planes[a]

atom	dev, Å	atom	dev, Å
O_1	0.005 (6)	C_4	0.017 (7)
O_2	0.016 (5)	C_5	0.003 (8)
C_1	−0.014 (7)	C_6	−0.024 (8)
C_2	−0.019 (6)	C_7	−0.024 (9)
C_3	−0.009 (6)	C_{11}	0.036 (11)

Twist Angles, Deg

octahedron	trigonal prism	$[Cr(O_2C_6H_4)_3]^{3-}$	$Cr[O_2C_6H_2(C_4H_9)_2]_3$
60	0	50.5 (6)	48.6 (7)

[a] Equation for the least-squares plane is $8.063x - 13.943y - 7.208z + 0.019 = 0$.

other C–C bonds in contrast to the $[Cr(cat)_3]^{3-}$ structure (vide infra). The chelate rings, including the central *tert*-butyl carbons, are strictly planar (see Table VI).

Results and Discussion

Structure. Since catechol–quinone is a non-innocent ligand system, assignment of chemically meaningful formal oxidation

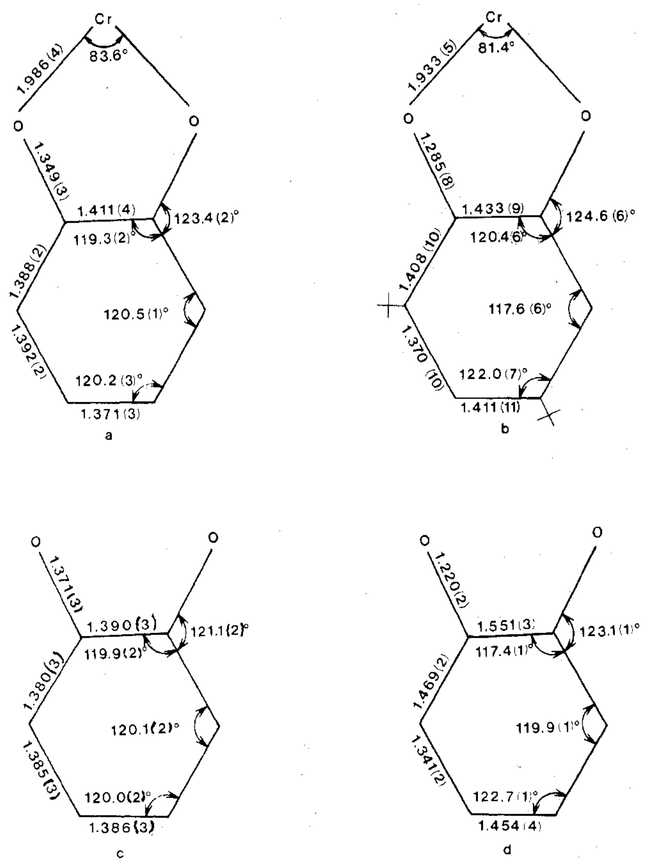

Figure 3. Schematic diagram for the structural comparison of (a) the trianion $[CrL_3]^{3-}$, (b) the neutral CrL_3, (c) catechol, and (d) *o*-benzoquinone.[1,32,33] The figure shows average bond distances (Å) and angles (deg).

states to the metal and ligand is to some extent without significance. However, the electronic structures and bonding of the CrL_3^{n-} complexes do pose chemical questions which have meaning. Any model for the bonding must explain the observed structural, magnetic, electrochemical, and spectroscopic properties of these materials. The diamagnetic neutral CrL_3 complex could be formulated as a Cr(0) complex of three quinone ligands, as a Cr(VI) complex of catechol dianion, or as a spin-coupled Cr(III) complex of three semiquinone radical anions. In valence bond terms these are all individual resonance forms of one electronic state. In molecular orbital terms the relative contribution of such formal oxidation states corresponds to assigning the relative contribution of metal and ligand atomic orbitals to the highest occupied molecular orbitals of the complex.

If one considers the coordination geometry to be essentially octahedral, the contribution of one filled σ AO and one empty π^* AO per oxygen makes the symmetry of the CrO_6 chromophore approximately T_d (since trans oxygen atom π orbitals are mutually perpendicular). This gives π^* symmetry orbitals from the oxygen which correspond to t_1 and t_2 representations, of which the latter can interact with the t_2 orbitals (d_{xy}, d_{xz}, d_{yz}) of the metal. In the neutral CrL_3 complex the total electron occupancy is six and this increases to nine in the trianion. Anything more than these qualitative features of the metal–ligand π interaction will have to await a more detailed and quantitative theoretical analysis; however, two main points about the bonding emerge from the structural details:

(1) The LUMO in CrL_3 is π antibonding since both the Cr–O and C–O bond lengths increase markedly on addition of three electrons to CrL_3 to give CrL_3^{3-} (see Figure 3).

(2) The geometry of the ligand in CrL_3 is much closer to a quinone structure than to catecholate.

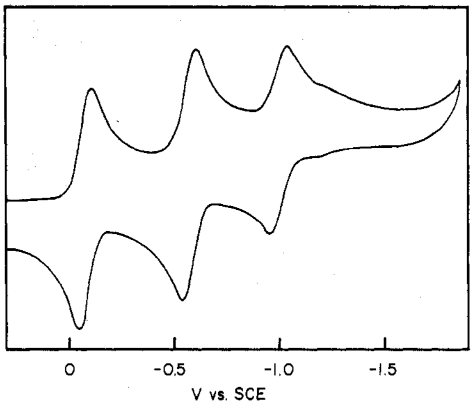

Figure 4. Cyclic voltammogram of a 10^{-3} M solution of the complexes of chromium and 3,5-di-*tert*-butylcatechol in acetonitrile containing 0.1 M tetraethylammonium perchlorate (scan rate, 100 mV/s at a platinum disk electrode vs. the SCE).

Bona fide metal(III)–catecholate complexes have C–O bond lengths of 1.35 Å,[1] catechol itself has a C–O bond length of 1.37 Å,[32] while in *o*-benzoquinone the C–O bond length is 1.22 Å.[33] The observed C–O distance in the di-*tert*-butyl-substituted neutral complex is 1.29 Å. Although this distance is less than the mean of C–O and C=O distances—where one might expect to find a semiquinone—it is pertinent to note that metal tropolonates and acetylacetonates have C–O bond distances averaging 1.28 Å. The geometry of the C_6 ring is closer to the quinone structure (Figure 3). Thus, while the C–C bond lengths in tris(catecholato)chromate(III) are 1.39 ± 0.02 Å, there is a substantial distortion of the ring in the neutral complex with the shortest bonds 1.370 (10) Å and the longest 1.433 (9) Å.

Electrochemistry, Magnetic Properties, and Spectra. The cyclic voltammogram of the complexes reported here is shown in Figure 4. For reversible *n*-electron couples, peak separations of 59/*n* mV are predicted at 25 °C.[34] By this criterion, the third reduction (far right wave in Figure 4) is quasi-reversible. Nevertheless, for all three waves, reduction potentials were calculated as the average of the peak potentials. Thus, moving from left to right on Figure 4 shows potentials of +0.03, −0.47, and −0.89 V vs. SCE corresponding to the **4** ↔ **5**, **5** ↔ **6**, and **6** ↔ **7** couples, respectively. In addition, two irreversible oxidation waves are observed at +0.96 and +1.13 V vs. SCE. Under identical conditions, 3,5-di-*tert*-butylcatechol has oxidation waves at +1.27 and +2.33 V vs. SCE. Cathodic electrolysis of the neutral complex in dry acetonitrile 0.2 V beyond the half-wave potentials generates, respectively, the blue monoanion, orange dianion, and pale green trianion from the red-violet starting material. In each case cyclic voltammetry of the electrolytically produced species gives a voltammogram identical with that shown in Figure 4. Controlled-potential electrolysis confirmed that each redox step is a one-electron process.

The electrochemical results are interpreted as follows: The quasi-reversible, nearly equally spaced reduction waves correspond to stepwise addition of electrons to molecular orbitals which are primarily ligand based. Likewise, the irreversible oxidations correspond to formation of a formal chromium(III) quinone, whereupon the neutral ligand dissociates from the metal.

The various species in the electron-transfer series may also be prepared chemically. Synthesis of the terminal members of the series is described in the Experimental Section. Molecular oxygen rapidly transforms the trianion to the monoanion even in the solid state. Upon prolonged exposure to O_2, the neutral species is formed. A 2:1 mixture of trianion and neutral complexes in THF smoothly affords the orange

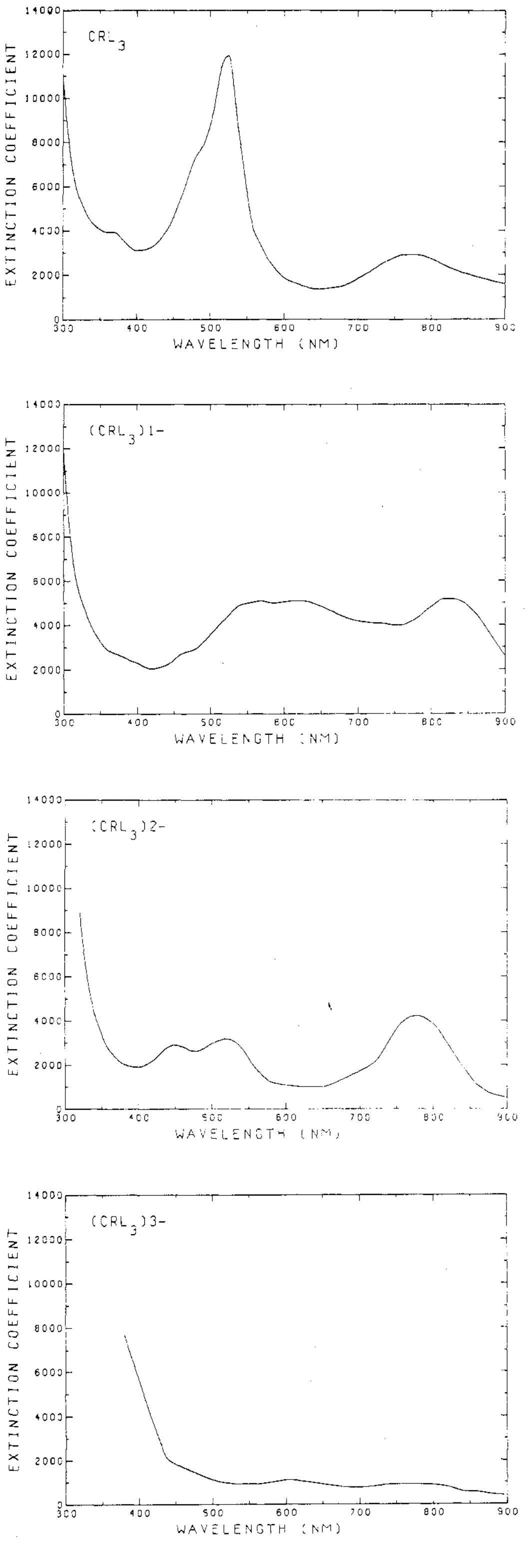

Figure 5. Visible spectra in acetonitrile of tris(3,5-di-*tert*-butylcatecholato)chromium(3–) ($[CrL_3]^{3-}$) and the oxidized species $[CrL_3]^-$, $[CrL_3]^{2-}$, and $[CrL_3]^0$.

dianion. Zinc amalgam, sodium naphthalide, and potassium metal all reduce the neutral species to the trianion. The recent work of Razuvaev et al.[7] is consistent with these observations. The system is therefore chemically as well as electrochemically reversible.

Aliquots of the electrolyzed solutions were withdrawn and studied by a variety of techniques. The optical spectra are shown in Figure 5. The fully reduced species, tris(3,5-di-*tert*-butylcatecholato)chromate(III) trianion (CrL_3^{3-}), has the familiar low-intensity spectrum typical of the spin-forbidden d–d bands of chromium(III) ion surrounded by six oxygen ligands. In the other members of this series any ligand field bands are obscured by intense charge-transfer bands of the complex which are primarily ligand π^* in origin but are even more intense than those of the free quinone or semiquinone. Electrochemical reduction of 3,5-di-*tert*-butylquinone in acetonitrile gives the semiquinone with visible absorption bands (approximate extinction coefficient) 760 (sh, 260), 665 (360), 433 (sh, 190), 380 (1680), and 342 (1840) nm. The free-quinone spectrum has absorption maxima at 570 (37) and 402 (1650) nm. (These results also indicate that the metal complexes have not decomposed significantly during electrolysis, which is consistent with the CV results for the electrolyzed solutions—vide supra.)

The solution susceptibilities of the chromium–catechol species were obtained by the Evans method at 25 °C. The neutral complex is diamagnetic. The electrochemically generated mono- and dianion have one unpaired electron [$\mu_{\text{eff}} = 1.9\ (1)\ \mu_B$] and two unpaired electrons [$\mu_{\text{eff}} = 2.7\ (1)\ \mu_B$], respectively. Of the neutral, monoanion, and dianion complexes only the monoanion yields an EPR spectrum between 298 and 77 K. The room-temperature spectrum in acetonitrile consists of a concentration-independent line at $g = 1.972$ with 8-G line width and coupling to the metal (^{53}Cr, $I = {}^3/_2$, 9.54% abundance) of 24.3 G. No proton hyperfine coupling was resolved. We interpret these magnetic data as further evidence that the redox processes occur on molecular orbitals with both significant ligand and metal character. In addition to the above solution studies, the magnetic susceptibility of the neutral species has been measured in the solid state at room temperature by the Gouy method and from 4.3 to 49 K using a vibrating-sample magnetometer. At all temperatures studied, the neutral complex is diamagnetic ($\chi_A = -1300 \times 10^{-6}$ cgsu mol^{-1}).

Infrared spectra of the neutral and trianion were recorded as hydrocarbon or fluorocarbon mulls since KBr pellets of the neutral complex were found to contain bands attributable to the free ligand. Chelation of the quinone to the metal shifts ν(C=C) from 1570 to 1575 cm^{-1}. While simple alkali metal salts of *p*-semiquinones show changes in intensity but not in position of C=O stretching bands compared to those of the parent quinones,[35] it is unlikely that these bands would remain unshifted in a chelated *o*-semiquinone. The C=O stretching bands appearing in the free quinone ligand around 1660 cm^{-1} are absent in the complexes. An intense new peak is observed at 1440 cm^{-1}. A similar observation was made for the $[Co(trien)(DBsq)]Cl_2$ complex.[8] This peak is absent in spectra of the fully reduced complex as well as both the catechol and quinone ligands. The strong band observed at 1250 cm^{-1} has previously been assigned to ν(C–O) in coordinated catechols;[36] however, as all of our complexes and both free quinones and catechols have strong bands at this energy, the band is of little diagnostic value. In agreement with Itoh et al., we assign ν(C–O) to 1367 cm^{-1} in the free-catechol ligand and to 1320 cm^{-1} in the trianion complex.[37] There is no peak in this region in the neutral complex.

In summary, we have prepared all members of the four-membered electron-transfer series bounded by tris(3,5-di-*tert*-butylcatecholato)chromate(III) and tris(3,5-di-*tert*-butyl-*o*-benzoquinone)chromium(0) [or tris(3,5-di-*tert*-butyl-*o*-benzosemiquinone)chromate(III)]. Members of this series have been investigated by X-ray diffraction and infrared, electronic, and EPR spectroscopies as well as magnetic susceptibility and electrochemical techniques. A small distortion toward trigonal-prismatic geometry in the neutral complex, the bond distances in the complex, and the electrochemical and magnetic experiments support the characterization of the neutral species as predominantly metal–quinoid in character and the trianion as a simple tris(catecholate) complex. Assignment of a formal oxidation state to the metal as the trianion is oxidized is largely ambiguous since the orbitals involved are delocalized over at least the metal and one ring.

Acknowledgment. We thank the NSF and, in part, the NIH for support of this research. We would like to thank Drs. Norman Edelstein and Derek Freyberg for experimental assistance.

Registry No. CrL_3^-, 68317-86-2; CrL_3^{2-}, 68317-87-3; CrL_3, 68366-30-3; $Cr(CO)_6$, 13007-92-6.

Supplementary Material Available: Tables IV and VII, structure factor amplitudes and root-mean-square amplitudes of vibration along principal axes (10 pages). Ordering information is given on any current masthead page.

References and Notes

(1) Raymond, K. N.; Isied, S. S.; Brown, L. D.; Fronczek, F. R.; Nibert, J. H. *J. Am. Chem. Soc.* **1976**, *98*, 1767–74.
(2) McCleverty, J. A. *Prog. Inorg. Chem.* **1968**, *10*, 49.
(3) Warren, L. F. *Inorg. Chem.* **1977**, *16*, 2814–9.
(4) Röhrscheid, F.; Balch, A. L.; Holm, R. H. *Inorg. Chem.* **1966**, *5*, 1542–51.
(5) Pierpont, C. G.; Downs, H. H. *J. Am. Chem. Soc.* **1976**, *98*, 4834–8, and references therein.
(6) Pierpont, C. G.; Buchanan, R. M.; Downs, H. H.; Shorthill, W. B. "Abstracts of Papers", 175th National Meeting of the American Chemical Society, Anaheim, Calif., 1978; American Chemical Society: Washington, D.C.; INOR 207.
(7) (a) Razuvaev, G. A.; Shal'nova, K. G.; Abakumova, L. G.; Abakumov, G. A. *Izv. Akad. Nauk, SSSR, Ser. Khim.* **1977**, 1642–5. (b) Lobanov, A. V.; Abakumov, G. A.; Razuvaev, G. A. *Dokl. Akad. Nauk SSSR* **1977**, 235, 824–7.
(8) Girgis, A. Y.; Sohn, Y. S.; Balch, A. L. *Inorg. Chem.* **1975**, *14*, 2327–31.
(9) Wicklund, P. A.; Beckmann, L. S.; Brown, D. G. *Inorg. Chem.* **1976**, *15*, 1996–7.
(10) Eisenberg, R. *Prog. Inorg. Chem.* **1970**, *12*, 295–369.
(11) Evans, D. F. *J. Chem. Soc.* **1959**, 2003–5.
(12) St. Räde, H. *J. Phys. Chem.* **1973**, *77*, 424.
(13) Mabbs, F. E.; Machin, D. J. "Magnetism and Transition Metal Complexes"; Chapman and Hall: London, 1973.
(14) Gleicher, G. J. "The Chemistry of the Quinoid Compounds", Vol. I, S. Patai, Ed.; Wiley: New York, N.Y., 1974; pp 13–7.
(15) "International Tables for X-ray Crystallography", Vol. II; Kynoch Press: Birmingham, England, 1960.
(16) The programs used for the PDP 8/E computer were those written by Enraf-Nonius Corp. In addition to local programs for the Lawrence Berkeley Laboratory CDC 7600 computer, the following programs or modifications were used: Zalkin's FORDAP Fourier program; Ibers' NUCLS, a group least-squares version of the Busing–Levy ORFLS program; ORFFE, a function and error program by Busing and Levy; and Johnson's ORTEP, a thermal ellipsoid plot program.
(17) The θ–2θ scan technique was used to collect intensity data for $\pm h,\pm k,\pm l$ to a 2θ angle of 40° and these data were averaged (R factor for averaging, 7.7% on F^2). For each reflection the scan angle was extended 25% on each side to estimate the background count. The scan time was variable with a maximum of 100 s. During data collection the intensities of the $22\bar{3}$, $\bar{2}1\bar{3}$, and $\bar{4}3\bar{1}$ reflections were measured as standards every 5400 s of X-ray exposure and showed no significant fluctuations. The intensities of three high-angle ($\theta = 26°$) orientation reflections were monitored every 200 reflections and a new orientation matrix was calculated if the setting angles had changed by more than 0.1° in any axis.
(18) An attenuator decreasing the intensity of the diffracted beam by a factor of 18.17 was automatically inserted into the beam when the prescan indicated an intensity too high for accurate counting. The θ scan angle was calculated as $(0.60 + 0.35 \tan \theta)$, and an aperture with a height of 4 mm and a variable width (width $= 2.50 + 0.50 \tan \theta$) was located 173 mm from the crystal.
(19) Abu-Dari, K. I.; Ekstrand, J. D.; Freyberg, D. P.; Raymond, K. N. *Inorg. Chem.*, **1979**, *18*, 108.
(20) In all refinements the function minimized was $\sum w(|F_o| - |F_c|)^2$, where F_o and F_c are the observed and calculated structure factors. The weighting factor, w, is $4F_o^2/\sigma^2(F_o^2)$. The atomic scattering factors for the nonhydrogen atoms were taken from the tabulations of Cromer and Mann.[21] Hydrogen scattering factors were those calculated by Stewart, Davidson, and Simpson.[22] Corrections for anomalous dispersion effects for the metal were made using $\Delta f'$ and $\Delta f''$ values of Cromer.[23]
(21) Cromer, D. T.; Mann, B. *Acta Crystallogr., Sect. A* **1968**, *24*, 321–4.
(22) Stewart, R. F.; Davidson, E. R.; Simpson, W. T. *J. Chem. Phys.* **1965**, *42*, 3175–87.
(23) Cromer, D. T. *Acta Crystallogr.* **1965**, *18*, 17–23.
(24) Churchill, M. R. *Inorg. Chem.* **1973**, *12*, 1213–4.
(25) $R = \sum ||F_o| - |F_c|| / \sum |F_o|$; $R_w = [\sum w(|F_o| - |F_c|)^2 / \sum w|F_o|^2]^{1/2}$. The error in an observation of unit weight is defined as $[\sum w((|F_o| - |F_c|)^2)/(N_{obsd} - N_{var})]^{1/2}$.
(26) Supplementary material.
(27) Avdeef, A.; Fackler, J. P., Jr. *Inorg. Chem.* **1975**, *14*, 2002–6.
(28) Muetterties, E. L.; Guggenberger, L. J. *J. Am. Chem. Soc.* **1974**, *96*, 1748–56.
(29) Abbreviations used in this paper: cat = catecholate dianion, Cl(cat) = tetrachlorocatecholate dianion, Cl(quin) = tetrachloro-*o*-benzoquinone, DBsq = 3,5-di-*tert*-butyl-*o*-benzosemiquinone, acac = acetylacetonate, SCE = saturated calomel electrode, EPR = electron paramagnetic resonance, trien = triethylenetetramine.
(30) Morosin, B. *Acta Crystallogr., Sect. B* **1965**, *19*, 131–7.
(31) van Niekerk, J. N.; Schoening, F. R. L. *Acta Crystallogr.* **1952**, *5*, 499–505.
(32) Wunderlich, H.; Mootz, D. *Acta Crystallogr., Sect. B* **1971**, *27*, 1684–6.
(33) Macdonald, A. L.; Trotter, J. *J. Chem. Soc., Perkin Trans. 2* **1973**, 476–80.
(34) Nicholson, R.; Shain, I. *Anal. Chem.* **1964**, *36*, 706–23.
(35) Matsunaga, Y. *J. Chem. Phys.* **1964**, *41*, 1609–13.
(36) Brown, D. G.; Reinprecht, J. T.; Vogel, G. C. *Inorg. Nucl. Chem. Lett.* **1976**, *12*, 399–404.
(37) Itoh, Y.; Nakahara, M.; Kondo, Y. *Nippon Kagaku Zasshi* **1971**, *92*, 227–33.